Article

High Performance Polymers

High Performance Polymers
1–10

DOI: 10.1177/0954008315617230
hip.sagepub.com

Synthesis and characterization of organosoluble, transparent, and hydrophobic fluorinated polyimides derived from 3,3′-diisopropyl-4,4′-diaminodiphenyl-4″-trifluoromethyltoluene

Chanjuan Liu[1,2], Xianglin Pei[1], Mei Mei[1], Guoquan Chou[1], Xiaohua Huang[1] and Chun Wei[1]

Abstract

A novel aromatic fluorinated diamine monomer, 3,3′-diisopropyl-4,4′-diaminodiphenyl-4″-trifluoromethyltoluene, was synthesized by coupling of 2-isopropylaniline and 4-(trifluoromethyl)benzaldehyde and its structure was confirmed by Fourier transform infrared spectroscopy, nuclear magnetic resonance, elemental analysis, and mass spectrometry, and then used to prepare a series of fluorinated polyimides (FPIs) by polycondensation reaction with various commercial dianhydrides via conventional one-step method. The obtained FPIs present excellent solubility in most organic solvents and enough to cast into tough and flexible films. All the FPI films show good optical transparency and light color with the cutoff wavelengths in range of 307–362 nm and the average transmittance above 86%. These polymer films also exhibit high glass transition temperature in range of 261–331°C and thermal stability with 10% weigh loss above 463°C under nitrogen atmosphere. Furthermore, they exhibit outstanding mechanical properties with tensile strengths of 65.9–94.3 MPa, elongation at break of 11.4–13.8%, Young's modulus of 1.6–1.9 GPa, and low dielectric constants in range of 2.75–3.10 at 1 MHz as well as prominent hydrophobicity with the contact angle in the range of 87.3–93.9°.

Keywords

Fluorinated polyimides, solubility, transparency, dielectric constant, hydrophobicity

Introduction

In the last few decades, polyimide (PIs) as a class of high-performance polymer materials have been growing steadily because of its excellent overall performance, such as thermo-oxidative stability, excellent mechanical strength, unique electrical properties, high radiation, solvent resistance, and hydrophobicity. So far, PIs have been applied to many fields including aerospace, microelectronic device, separation techniques, polymer electrolyte fuel, and so on.[1–6] However, conventional aromatic PIs presented poor solubility in most common solvents, high processing temperature, and deep reddish-brown coloration due to rigid chains and strong interchain interactions, which further limited their applications in many fields.

In order to overcome these drawbacks as mentioned above and balance the thermal stability and the processability, many efforts have been made to improve the processing characteristics and strong color. Currently, one of the effective methods included chemical structure modifications, such as incorporation of flexible linkages, bulky pendant groups, dendronized and hyperbranched structure, noncoplanar structure, spiro skeleton linkages, unsymmetrical

[1] Key Laboratory of New Processing Technology for Nonferrous Metal and Materials, Ministry of Education, and School of Material Science and Engineering, Guilin University of Technology, Guilin, People's Republic of China
[2] Ministry of Education Key Laboratory for the Chemistry and Molecular Engineering of Medicinal Resources, School of Chemistry and Pharmaceutical Science, Guangxi Normal University, Guilin, People's Republic of China

Corresponding author:
Xiaohua Huang, Key Laboratory of New Processing Technology for Nonferrous Metal and Materials, Ministry of Education, School of Material Science and Engineering, Guilin University of Technology, Guilin, People's Republic of China.
Email: huangxiaohua@glut.edu.cn

structure, and acyclic moieties into the diamine and/or dianhydride fragment.[7–22] Moreover, one of the most promising methods to obtain solubility and thermoplasticity of PIs is the introduction of pendant fluoro and trifluoromethyl groups. It is well known that fluorinated polyimide (FPIs) presented excellent solubility, outstanding mechanical properties, good thermal stability, high optical transparency, prominent hydrophobicity, low dielectric constants, low birefringence, and low refractive index.[23–29] These overall properties of FPIs are attributed to the special characteristics of fluorine, such as small dipole, high electron negativity, oxidization resistance, hydrophobicity, and low polarizability. Tapaswi et al.[28] designed and synthesized two new perfluorodecylthio-substituted aromatic diamines, 2,4-diamino-1-(1*H*,1*H*,2*H*,2*H*-perfluorodecathio)benzene and 2,2′-bis((1*H*,1*H*,2*H*,2*H*-perfluorodecyl)thio)(1,1′-biphenyl)4,4′-diamine, and then polycondensed with 4,4′-(hexafluoroisopropylidene)diphthalic anhydride (6FDA) to prepare two new perfluorinated PIs. The obtained polymers exhibited excellent solubility in common solvents, such as *N*-methyl-2-pyrrolidinone (NMP), *N*,*N*-dimethylacetamide (DMAc), *N*,*N*-dimethylformamide (DMF), dimethyl sulfoxide (DMSO), acetone, toluene, xylene, chloroform ($CHCl_3$) and tetrahydrofuran (THF), high optical transparency, hydrophobicity, low dielectric constant, and thermo-mechanical stabilities due to the presence of the perfluorodecylthio side group in the polymer chain. Yang et al.[29] synthesized a fluorinated diamine monomer with a *tert*-butyl group, 4-*tert*-butyl-[1,2-bis(4-amino-2-trifluoromethylphenoxy)phenyl] benzene, and polymerized it with various aromatic tetracarboxylic acid dianhydrides. These polymers showed well solubility in common solvents such as NMP, DMAc, DMF, DMSO, *m*-cresol, pyridine, dioxane, THF, dichloromethane, and acetone, as well as lower color intensity, dielectric constant, and moisture absorption.

In this article, the solubility and optical transparency of PIs are expected to be improved by incorporation of bulky pendant substituent, trifluoromethyl groups and noncoplanar structure in the polymer chain. Hence, a novel aromatic diamine monomer, 3,3′-diisopropyl-4,4′-diaminodiphenyl-4″-trifluoromethyltoluene (PAPFT), is designed and synthesized and then used to prepare a series of FPIs containing isopropyl and trifluoromethyl in the main chain with various commercially aromatic dianhydrides. The solubility, optical transparency, thermal stability, tensile strengths, dielectric properties, and hydrophobicity of FPIs were investigated.

Experimental procedure

Materials

4-(Trifluoromethyl)benzaldehyde (Shanghai Darui Chemical Co., Ltd, China) and 2-isopropylaniline (Sigma-Aldrich, St Louis, Missouri, USA) were used as received. Pyromellitic dianhydride (PMDA) (Shanghai Guoyao Chemical Co., Ltd, China), 3,3′,4,4′-biphenyltetracarboxylic dianhydride (BPDA), 4,4′-oxydiphthalic anhydride (ODPA) (Changzhou Linchuan Chemical Co., Ltd, China), 3,3′,4,4′-benzophenone tetracarboxylic dianhydride (BTDA), and 4,4′-(hexafluoroisopropylidene)-diphthalic anhydride (6FDA) (Tokyo Chemical Industry Co., Ltd, Japan) were recrystallized from acetic anhydride. DMF was purified by refluxing with calcium hydride, distilled under reduced pressure before use. All other reagents and solvents were used without any further purification.

Measurements

The proton nuclear magnetic resonance (^{1}H NMR) and carbon 13 NMR (^{13}C NMR) spectra were measured on a 400 MHz Bruker instrument (Billerica, Massachusetts, USA) with deuterated DMSO (DMSO-d_6) as solvent and tetramethylsilane as internal standard. The Fourier transform infrared (FTIR) spectrum (potassium bromide; KBr) was surveyed on a Thermo Nexus 470 FTIR spectrometer (Fitchburg, Wisconsin, USA). Elemental analysis was tested on a PerkinElmer model 2400 II system (Waltham, Massachusetts, USA). Mass spectrometry was measured on an Elementar Vario EL III/Isoprime (Germany). Differential scanning calorimetry (DSC) was recorded on a NETZSCH 204 DSC instrument at a heating rate of 10°C min^{-1} under nitrogen atmosphere. Thermogravimetric analysis (TGA) was determined in a TGA Q500 analyzer at a heating rate of 10°C min^{-1} under nitrogen atmosphere. Gel permeation chromatography (GPC) was performed on a Waters 1515 analyzer (New Castle, Delaware, USA) relative to polystyrene standard using DMF as the eluent. Ultraviolet–visible (UV-Vis) spectrum was conducted on a 3600 UV-Vis spectrophotometer at room temperature. Dielectric constant was investigated by the parallel plate capacitor method using a dielectric analyzer (Agilent 4294A, Santa Clara, California, USA) on thin film. Gold electrode was deposited by vacuum coating on both surfaces of film, and FPI films were determined in a dry chamber at the frequency of 1 MHz. The mechanical properties of the films were measured using AG-I 50 KN (Kyoto, Japan) and the size of each film was about $50 \times 5 \times 0.05$ mm^3. The contact angle of the polymer film for water was carried on a JY-PHb (Chengde, Hebei, China) contact angle analysis system.

Monomer synthesis

3,3′-diisopropyl-4,4′-diaminodiphenyl-4″-trifluoromethyltoluene. A 250 mL three-necked flask equipped with a magnetic stirrer, a condenser and a dropping funnel was charged with 2-isopropylaniline (48.70 g, 0.36 mol). The solution was stirred at 120°C for 0.5 h under nitrogen atmosphere and then the mixture of 4-(trifluoromethyl)benzaldehyde (25.30 g, 0.14 mol) and 7.5 mL (12 N) hydrochloric acid

was added through a dropping funnel over 1 h, and then continued to stir about 30 min. The mixture was heated to 150°C for 10 h, and then the mixture solution was cooled to room temperature, and 80 mL 10% aqueous solution of sodium hydroxide was added. After the excess hydrochloric acid was neutralized, the mixture solution was extracted by moderate dichloromethane and washed with deionized water several times until pH value of solution was neutral. Finally, after evaporation, the obtained crude product was further purified by silica gel chromatography with ethyl acetate and petroleum ether (1:4, v/v) as mixed eluent (32.84 g, yield 55%); melting point 107°C (by DSC at a scan rate of 5°C min^{-1}).

^{1}H NMR (δ, ppm, DMSO-d_6): 7.59 (d, 2 H, J=4.8 Hz), 7.26 (d, 2 H, J=6.2 Hz), 6.78 (s, 2 H), 6.56 (m, 4 H), 5.29 (s, 1 H), 4.72 (s, 4 H, NH_2), 2.88–2.94 (m, 2 H), 1.04 (d, 12 H, J=5.8 Hz); ^{13}C NMR (δ, ppm, DMSO-d_6): 151.78, 144.08, 132.14, 131.62, 130.18, 127.24, 126.10, 125.46, 123.79, 121.48, 115.35, 55.60, 27.08, 23.04; FTIR (KBr, cm^{-1}): approximately 3500–3200 cm^{-1} (-NH_2, br, vs), approximately 3000–2800 cm^{-1} (C–H, br, s), 1066 cm^{-1} (–CF_3, s); Elemental analysis calculated for PAPFT ($C_{26}H_{29}F_3N_2$): C, 73.22%; N, 6.57%. Found: C, 72.50%; N, 6.88%; MS (m/z): 427.2 ([M+H]$^+$).

Polymer synthesis

All PIs were synthesized by one-step process. PI-ODPA prepared from PAPFT and ODPA as a typical case and the experimental procedure was as described below. A 50 mL three-necked flask equipped with a condenser, mechanical stirrer, and nitrogen gas inlet tube was charged with PAPFT (0.9607 g, 2.25 mmol), ODPA (0.6987 g, 2.25 mmol), *m*-cresol (14.65 g, 14.5 mL) and about five drops of isoquinoline. Firstly, the mixture was stirred at room temperature under nitrogen atmosphere to remove residual air until the monomers dissolved completely. Then, ladder-elevating temperature was conducted with 80°C for 4 h, 120°C for 4 h and 200°C for 10 h. After that, the mixture was cooled and then precipitated by pouring into 450 mL ethanol to get light yellow fibers, and then filtered, washed with ethanol several times, and dried overnight under vacuum at 150°C. The obtained light yellow fibrous precipitate was dissolved in DMF, and then poured into alcohol for further purification at least twice. The synthetic procedure of PI-PMDA (PAPFT-PMDA), PI-BPDA (PAPFT-BPDA), PI-BTDA (PAPFT-BTDA), and PI-6FDA (PAPFT-6FDA) were similar to the synthetic procedure of PI-ODPA.

PI-PMDA. Yield, 93%. FT-IR (KBr, cm^{-1}): approximately 3068–2871 cm^{-1} (alkyl, br, vs), 1779 cm^{-1} and 1727 cm^{-1} (C=O, vs, imide, stretching vibration), 1371 cm^{-1} (C-N, vs), 729 cm^{-1} (C=O, s, imide, bending vibration). ^{1}H NMR (400 MHz, DMSO-d_6, ppm): 8.42 (d, 2 H, J = 5.2 Hz, ArH), 7.76 (d, 2 H, J = 8.4 Hz, ArH), 7.49 (d, 2 H, J = 8.0 Hz, ArH), 7.35–7.43 (m, 4 H, ArH), 7.19 (d, 2 H, J = 4.0 Hz, ArH), 5.98 (s, 1 H, CH), 2.79–2.85 (m, 2 H, $CH(CH_3)_2$), 1.05 (d, 12 H, J = 6.4 Hz, CH_3). Elemental analysis calculated for $(C_{36}H_{27}F_3N_2O_4)_n$: C, 71.05%; N, 4.60%. Found: C, 72.14%; N, 4.55%.

PI-BPDA. Yield, 95%. FTIR (KBr, cm^{-1}): approximately 3060–2870 cm^{-1} (alkyl, br, vs), 1777 cm^{-1} and 1727 cm^{-1} (C=O, vs, imide, stretching vibration), 1374 cm^{-1} (C–N, vs), 742 cm^{-1} (C=O, s, imide, bending vibration). ^{1}H NMR (400 MHz, DMSO-d_6, ppm): 8.42–8.36 (m, 4 H, ArH), 8.08 (d, 2 H, J = 4.8 Hz, ArH), 7.74 (d, 2 H, J = 6.4 Hz, ArH), 7.48 (d, 2 H, J = 7.6 Hz, ArH), 7.30–7.36 (m, 4 H, ArH), 7.15 (d, 2 H, J = 8.8 Hz, ArH), 5.96 (s, 1 H, CH), 2.77–2.82 (m, 2 H, $CH(CH_3)_2$), 1.05 (d, 12 H, J = 5.6 Hz, CH_3). Elemental analysis calculated for $(C_{42}H_{31}F_3N_2O_4)_n$: C, 73.67%; N, 4.09%. Found: C, 73.18%; N, 4.18%.

PI-ODPA. Yield, 94%. FT-IR (KBr, cm^{-1}): approximately 3067–2870 cm^{-1} (alkyl, br, vs), 1779 cm^{-1} and 1727 cm^{-1} (C=O, vs, imide, stretching vibration), 1375 cm^{-1} (C–N, vs), 748 cm^{-1} (C=O, s, imide, bending vibration). ^{1}H NMR (400 MHz, DMSO-d_6, ppm): 8.03 (d, 2 H, J = 8.0 Hz, ArH), 7.72 (d, 2 H, J = 8.4 Hz, ArH), 7.62–7.64 (m, 4 H, ArH), 7.46 (d, 2 H, J = 8.0 Hz, ArH), 7.29–7.31 (m, 4 H, ArH), 7.12 (d, 2 H, J = 8.0 Hz, ArH), 5.93 (s, 1 H, CH), 2.74–2.81 (m, 2 H, $CH(CH_3)_2$), 1.02 (d, 12 H, J = 1.2 Hz, CH_3). Elemental analysis calculated for $(C_{42}H_{31}F_3N_2O_5)_n$: C, 71.99%; N, 4.00%. Found: C, 70.05%; N, 4.12%.

PI-BTDA. Yield, 93%. FT-IR (KBr, cm^{-1}): approximately 3067–2870 cm^{-1} (alkyl, br, vs), 1779 cm^{-1} and 1724 cm^{-1} (C=O, vs, imide, stretching vibration), 1372 cm^{-1} (C–N, vs), 725 cm^{-1} (C=O, s, imide, bending vibration). ^{1}H NMR (400 MHz, DMSO-d_6, ppm): 8.25 (d, 2 H, J = 7.2 Hz, ArH), 8.18 (d, 2 H, J = 10 Hz, ArH), 7.68–7.76 (m, 4 H, ArH), 7.46 (d, 2 H, J = 6.8 Hz, ArH), 7.28–7.37 (m, 4 H, ArH), 7.14 (d, 2 H, J = 8.4 Hz, ArH), 5.92 (s, 1 H, CH), 2.79–2.83 (m, 2 H, $CH(CH_3)_2$), 1.03 (d, 12 H, J = 2.4 Hz, CH_3). Elemental analysis calculated for $(C_{43}H_{31}F_3N_2O_5)_n$: C, 72.46%; N, 3.93%. Found: C, 73.05%; N, 3.75%.

PI-6FDA. Yield, 92%. FTIR (KBr, cm^{-1}): approximately 3070–2872 cm^{-1} (alkyl, br, vs), 1786 cm^{-1} and 1727 cm^{-1} (C=O, vs, imide, stretching vibration), 1375 cm^{-1} (C–N, vs), 724 cm^{-1} (C=O, s, imide, bending vibration). ^{1}H NMR (400 MHz, DMSO-d_6, ppm): 8.14 (d, 2 H, J = 5.6 Hz, ArH), 7.93 (d, 2 H, J = 6.4 Hz, ArH), 7.69–7.80 (m, 4 H, ArH), 7.45 (d, 2 H, J = 9.6 Hz, ArH), 7.27–7.32 (m, 4 H, ArH), 7.11 (d, 2 H, J = 8.0 Hz, ArH), 5.91 (s, 1 H, CH), 2.79–2.84 (m, 2 H, $CH(CH_3)_2$), 1.00 (d, 12 H, J = 5.6 Hz, CH_3). Elemental analysis calculated for $(C_{45}H_{31}F_9N_2O_4)_n$: C, 64.75%; N, 3.36%. Found: C, 64.25%; N, 3.42%.

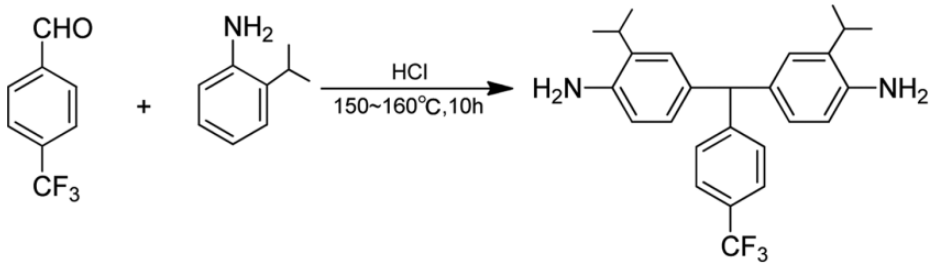

Figure 1. Synthesis of diamine monomer PAPFT. PAPFT: 3,3′-diisopropyl-4,4′-diaminodiphenyl-4′′-trifluoromethyltoluene.

Polyimide film preparation

In order to prepare transparent and homogeneous thin films for testing the optical properties, thermal properties, mechanical properties, and hydrophobicity and dielectric constants of PI, the polymers were dissolved in DMF with a concentration of about 2 wt% and 10 wt%, respectively. Then the obtained homogeneous solution was poured onto a dry and clean glass plate, and then heated at 60°C for 24 h. After most of DMF evaporated, the polymer films were prepared after self-stripped off from the glass surface by soaking in water, and then heated at 180°C under vacuum for 12 h.

Results and discussion

Monomer synthesis

The synthetic route of fluorinated diamine PAPFT is shown in Figure 1. The chemical structures of the monomer were characterized by FTIR, NMR, elemental analysis, and mass spectrometry (MS). The FTIR spectra showed that the absorption peaks approximately around 3500–3200 cm^{-1} ascribed to the $–NH_2$ groups, the characteristic absorption peaks of the alkyl groups appeared at approximately 3000–2800 cm^{-1}, and the peaks at about 1066 cm^{-1} assigned to the C–F bonds. The NMR spectrum of the monomer was illustrated in Figure 2. Obviously, the characteristic signals of aromatic protons appeared in the range of approximately 7.59–6.56 ppm, the peak at 4.72 ppm corresponded to amine groups ($–NH_2$), and the protons of alkyl (–CH–, $–CH(CH_3)_2$, $–CH_3$) protons were indicated at 5.29, 2.91, and 1.04 ppm, respectively. Meanwhile, the ^{13}C NMR spectrum showed 14 obvious signal peaks in the area of approximately 151.78–23.04 ppm. The assignment of total protons in the spectrum was consistent with the proposed chemical structure of polymer. Furthermore, combining with the results of MS spectrometry and element analysis, the results were also accorded with the proposed structure.

Polymer synthesis

A series of FPIs were prepared with PAPFT and five commercially aromatic dianhydrides *via* one-step high-temperature polycondensation procedure and the reaction route is shown in Figure 3. The structures of polymer were confirmed by GPC, FTIR, ^1H NMR, and elemental analysis. The FTIR spectra showed the characteristic absorption peaks of alkyl groups at approximately 3070–2870 cm^{-1}, imide carbonyl at around 1780 cm^{-1} and 1725 cm^{-1}, C–N at about 1375 cm^{-1}, and imide ring at about 730 cm^{-1} (Figure 4). Moreover, the characteristic peaks of the $–NH_2$ groups disappeared at approximately 3500–3200 cm^{-1}, which indicated that the imidization reaction was completed. As a typical example, the ^1H NMR spectrum of the PI-ODPA is illustrated in Figure 5. The assignments of all the protons were in complete agreement with the assumed structure. Combined with the elemental analysis values (Table 1), the obtained polymers were consistent with the proposed polymer structure. The results of GPC are also illustrated in Table 1, the obtained FPIs presented higher number-average molecular weight (M_n) and weight-average molecular weight (M_w) in the range of approximately 4.7×10^4–7.5×10^4 g mol^{-1} and 2.3×10^5–5.6×10^5 g mol^{-1}, respectively, and the lower polydispersity index (M_w/M_n) was in range of 4.1–7.5.

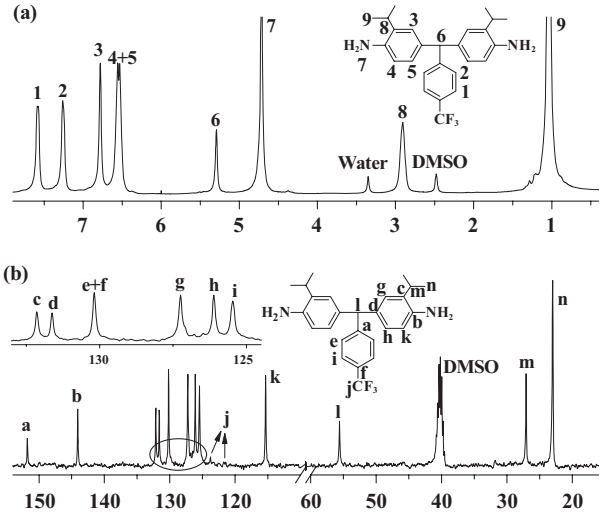

Figure 2. ^1H NMR (a) and ^{13}C NMR (b) spectra of diamine. ^1H NMR: proton nuclear magnetic resonance; ^{13}C NMR: carbon nuclear magnetic resonance.

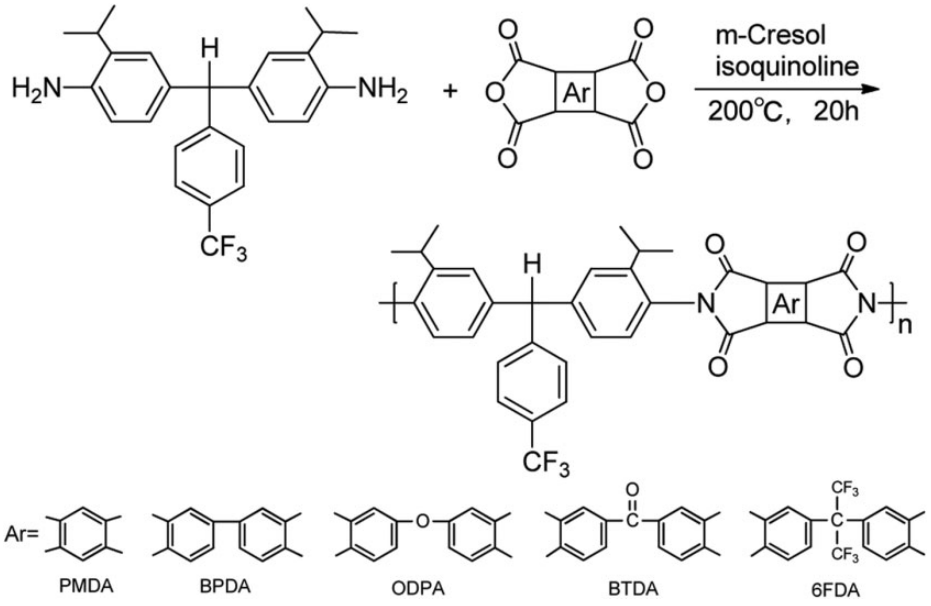

Figure 3. Synthesis of FPIs. FPIs: fluorinated polyimides.

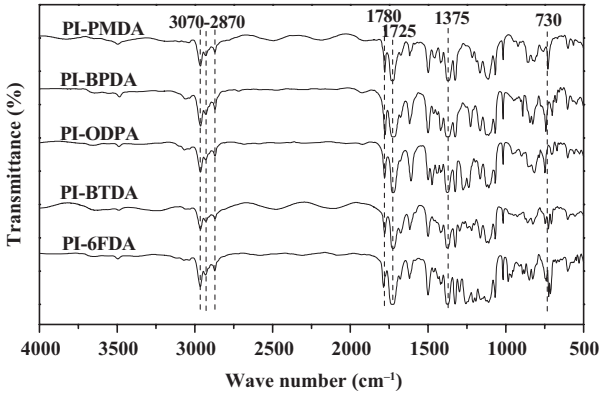

Figure 4. FTIR spectra of FPI films. FTIR: Fourier transform infrared; FPI: fluorinated polyimides.

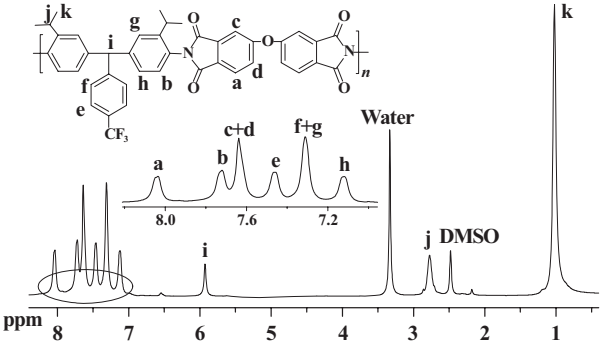

Figure 5. ^{1}H NMR spectra of polyimide PI-ODPA. ^{1}H NMR: proton nuclear magnetic resonance; PI: polyimide; ODPA: 4,4′-oxydiphthalic anhydride.

Table 1. GPC data and elemental analyses of FPIs.

	GPC data[a]			Elemental analysis (%)			
Polymer	$M_n \times 10^4$	$M_w \times 10^5$	M_w/M_n	Formula		C	N
PI-PMDA	6.8	3.4	5.0	$(C_{36}H_{27}F_3N_2O_4)_n$	Calculated	71.05	4.60
					Found	72.14	4.55
PI-BPDA	7.5	5.6	7.5	$(C_{42}H_{31}F_3N_2O_4)_n$	Calcd	73.67	4.09
					Found	73.18	4.18
PI-BTDA	5.5	3.5	6.4	$(C_{42}H_{31}F_3N_2O_5)_n$	Calcd	71.99	4.00
					Found	70.05	4.12
PI-ODPA	5.6	2.3	4.1	$(C_{43}H_{31}F_3N_2O_5)_n$	Calcd	72.46	3.93
					Found	73.05	3.75
PI-6FDA	4.7	3.3	7.0	$(C_{45}H_{31}F_9N_2O_4)_n$	Calcd	64.75	3.36
					Found	64.25	3.42

M_w: weight-average molecular weight; M_n: number-average molecular weight; PI: polyimide; PMDA; pyromellitic dianhydride; BPDA: 3,3′,4,4′-biphenyltetracarboxylic dianhydride; BTDA: 3,3′,4,4′-benzophenone tetracarboxylic dianhydride; ODPA: 4,4′-oxydiphthalic anhydride; 6FDA: 4,4′-(hexafluoroisopropylidene)-diphthalic anhydride.

[a]Relative to polystyrene standards, using DMF as the eluent.

Table 2. Solubility of FPIs.[a]

Polymer	Solvent								
	DMF	DMAc	DMSO	NMP	*m*-Cresol	$CHCl_3$	Acetone	THF	*n*-Hexane
PI-PMDA	++	++	++	++	++	++	++	++	− −
PI-BPDA	++	++	++	++	++	++	− −	+h	− −
PI-BTDA	++	++	++	++	++	++	++	++	− −
PI-ODPA	++	++	++	++	++	++	++	++	− −
PI-6FDA	++	++	++	++	++	++	++	++	− −

PMDA; pyromellitic dianhydride; BPDA: 3,3′,4,4′-biphenyltetracarboxylic dianhydride; BTDA: 3,3′,4,4′-benzophenone tetracarboxylic dianhydride; ODPA: 4,4′-oxydiphthalic anhydride; 6FDA: 4,4′-(hexafluoroisopropylidene)-diphthalic anhydride; DMF, *N,N*-dimethylformamide; DMAc: *N, N*-diethylformamide; DMSO, dimethyl sulfoxide; NMP, *N*-methyl-2-pyrrolidone. $CHCl_3$, chloroform; THF, tetrahydrofuran.
[a]Solubility was tested with a polymer concentration of 10 mg/mL in solvent with stirring.++: soluble at room temperature; +h: soluble on heating at 60°C; − −: insoluble.

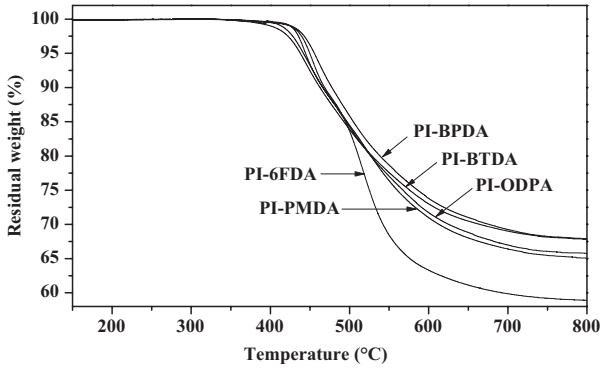

Figure 6. TGA curves of FPIs. TGA: thermogravimetric; FPIs: fluorinated polyimides.

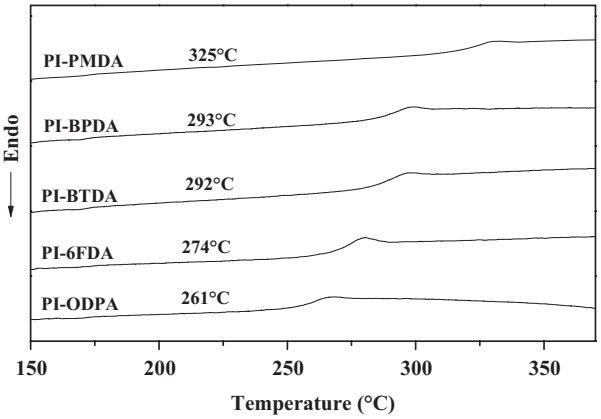

Figure 7. DSC curves of FPIs. DSC: differential scanning calorimetric; FPIs: fluorinated polyimides.

Solubility

The solubility of polymers was determined at a concentration of 10 mg mL^{-1} in various organic solvents and the results are summarized in Table 2. Compared to reported PIs, the prepared FPIs exhibited excellent solubility in strong dipolar solvents such as DMF, DMAc, NMP, DMSO, and *m*-cresol at room temperature. Furthermore, they could also be partially dissolved in low boiling point organic solvents such as $CHCl_3$, THF, and acetone at room temperature or upon heating. The excellent solubility of the obtained FPIs mainly attributes to the introduction of the bulky isopropyl and bulky pendent 4-trifluoromethylphenyl groups in the main chains, which increased the disorder of the polymer chains and hindered the dense of chain staking, and then decreased the intermolecular interactions and led to increased solubility. It was obvious that PI-BPDA was not soluble in acetone even on heating, and it may be due to the relatively large rigidity and the higher molecular weight of the polymer chains.

Thermal Properties

DSC and TGA techniques were applied to evaluate the thermal properties of the FPIs at a heating rate of 10°C min^{-1} under nitrogen atmosphere. The curves are illustrated in Figure 6 and 7, and the corresponding results are summarized in Table 3. It was apparent that the FPIs showed good thermal stability. The temperature at 5% and 10% weight loss were 438–456°C and 463–478°C, respectively. Meanwhile, the onset decomposition temperature of polymers was more than 416°C and the char yield was beyond 59% at 800°C. Furthermore, all the resulting FPIs presented high glass transition temperature (T_g) and the values of T_g were in range of 261–331°C. The high T_g values of FPIs were mainly ascribed to the large rigidity of inherent imide ring structure of the main chain. Meanwhile, the introduction of the bulky isopropyl and pendent 4-trifluoromethylphenyl groups in the polymer backbone caused a lowering of the chain's distorted mobility and thereby an increase in T_g. Moreover, the high-energy bond of the C–F in trifluoromethyl groups would make the polymer possess high T_g and thermal properties. PI-PMDA originated from PMDA presented the highest T_g due to the structure of the rigid pyromellitic units in the polymer chain. Predictably, PI-ODPA derived from ODPA showed the lowest T_g because of the introduction of flexible ether units in the polymer backbone.

Table 3. Thermal and optical properties of FPIs.

Polymer	T_g (°C)[a]	T_d (°C)[b]	$T_{5\%}$ (°C)[c]	$T_{10\%}$ (°C)[c]	Char yield (%)[d]	λ_{cutoff} (nm)	Transparency (%)[e]
PI-PMDA	331	419	442	466	65	326	86
PI-BPDA	295	437	456	478	68	362	88
PI-BTDA	261	428	444	466	66	339	89
PI-ODPA	292	416	438	463	68	335	87
PI-6FDA	274	458	450	469	59	307	90
LaRC™-CP1[f]	–	–	–	–	–	–	88
Kapton[g]	–	–	–	–	–	400	69

PMDA; pyromellitic dianhydride; BPDA: 3,3′,4,4′-biphenyltetracarboxylic dianhydride; BTDA: 3,3′,4,4′-benzophenone tetracarboxylic dianhydride; ODPA: 4,4′-oxydiphthalic anhydride; 6FDA: 4,4′-(hexafluoroisopropylidene)-diphthalic anhydride; TGA: thermogravimetric analysis.
[a]Glass transition temperature, obtained from DSC at a heating rate of 10°C min^{-1} in N_2.
[b]Onset decomposition temperature, obtained from TGA at a heating rate of 10°C min^{-1} in N_2.
[c]Temperature at 5% and 10% weight loss recorded by TGA at a heating rate of 10°°C min^{-1} in N_2.
[d]Char yield (wt%) at 800°C in N_2.
[e]Average percent transmission 400–780 nm.
[f]Data from Nexolve Co.
[g]According to the literature.[30]

Optical properties

As shown in Figure 8, the optical properties of FPI films were evaluated by UV-Vis spectra with the thickness of *ca.* 15–25 μm, and the corresponding resulting data are summarized in Table 3. The obtained FPI films presented higher optical transparency with cutoff wavelengths in range of 307–362 nm. Meanwhile, the transparency in the visible light region was investigated by averaging the transmittances in the wavelength range of 400–780 nm. The data showed that the average transmittance of FPI films was scope of 86–90%. According to the literature,[30] the average transmittance of prepared FPI films was better than that of commercial Kapton film with similar thickness (average transmittance, 69%). Furthermore, it is well known that LaRC™-CP1 film exhibits the lowest color of all commercially available PIs, and the average transmittance in the visible region (400–780 nm) is 88% with the thickness of 25 μm. By comparing optical transparency of LaRC™-CP1, these obtained FPI films presented excellent optical transparency, which made them have great advantage on the applications of optoelectronic device, displays, and aerospace applications. Moreover, compared the standard commercial Kapton film (Figure 9) with the thickness of *ca.* 45 μm, the FPI films were almost transparent with similar thickness in the visible region. The good optical transparency and light color may be due to the bulky substituents (isopropyl, 4-trifluoromethylphenyl) and the distorted noncoplanar structures in the polymer chains, which increased the free volume, and then reduced the inter- and intramolecular conjugation effect and restricted the charge transfer complex (CTC) formation between the diamine donor and dianhydride acceptor moieties. Furthermore, combined with the special characteristics of fluorine, such as high electron negativity, low polarizability, and a relatively larger free volume, the prepared FPI films presented higher transparency and lighter color. Apparently,

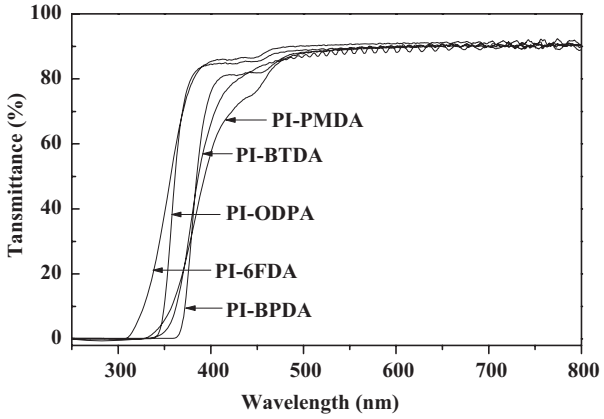

Figure 8. UV-Vis spectra of FPI films. UV: ultraviolet; Vis: visible; FPIs: fluorinated polyimides.

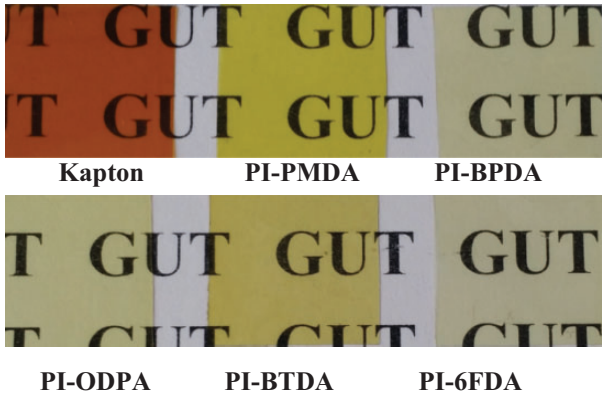

Figure 9. The profile images of FPI films. FPIs: fluorinated polyimides.

PI-ODPA and PI-6FDA films presented a lighter color (Figure 9), and it may be due to the introduction of the flexible ether units (ODPA) and fluorine-containing groups

Table 4. Mechanical properties, dielectric constants and hydrophobicity of FPI films.

Polymer	Tensile strength (MPa)	Elongation at break (%)	Young's modulus (GPa)	Dielectric constant at 1 MHz	Contact angle (°)
PI-PMDA	65.9	12.6	1.7	3.03	87.3
PI-BPDA	71.0	11.4	1.6	2.96	89.1
PI-ODPA	91.8	13.6	1.9	2.83	89.4
PI-BTDA	94.3	13.8	1.7	3.10	87.7
PI-6FDA	69.4	11.6	1.7	2.75	93.9
Kapton	–	–	–	3.48[a]	81.6[b]

PMDA; pyromellitic dianhydride; BPDA: 3,3′,4,4′-biphenyltetracarboxylic dianhydride; BTDA: 3,3′,4,4′-benzophenone tetracarboxylic dianhydride; ODPA: 4,4′-oxydiphthalic anhydride; 6FDA: 4,4′-(hexafluoroisopropylidene)-diphthalic anhydride.
[a]According to the literature.[9]
[b]Prepared in our laboratory.

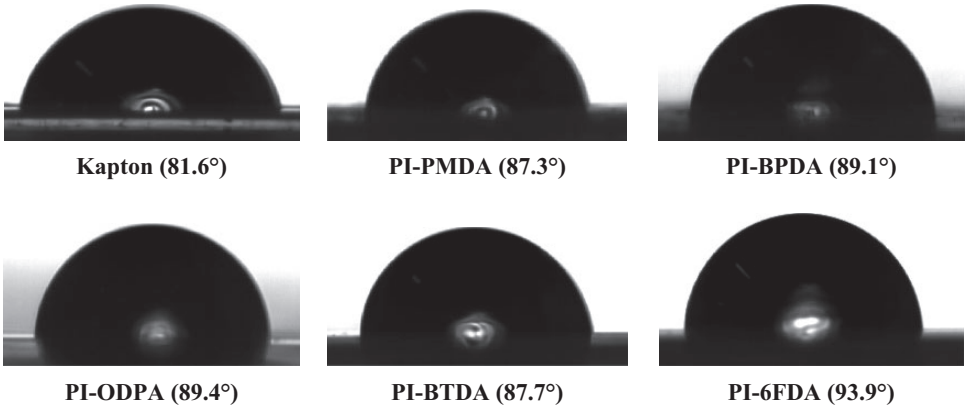

Figure 10. The profiles of a water droplet on the Kapton and FPI films. FPIs: fluorinated polyimides.

(6FDA) in the polymer backbone, which further reduced the formation of the inter- and intra-molecular CTC. The outstanding optical properties of the polymers make them have potential applications in the area of optical waveguides and optoelectronic devices.[31,32]

Mechanical properties and dielectric constants

The flexible and tough FPI films were prepared by casting method, and the thickness of the obtained films was at *ca.* 50 μm. The mechanical properties of FPIs were measured and summarized in Table 4. All the polymers presented excellent mechanical properties. The tensile strength of PI films was in range of 65.9–94.3 MPa, elongation at break in range of 11.4–13.8%, and young's modulus in range of 1.6–1.9 GPa, respectively. Meanwhile, the dielectric properties of FPI films were evaluated at the frequency of 1 MHz. As is known to all, low dielectric properties of the polymer played an important role in the application for microelectronics technology. As shown in Table 4, the dielectric constants of the obtained FPIs were in range of 2.75–3.10 at 1 MHz, which were lower than that of the commercial Kapton film (3.48 at 1 MHz). The prominent dielectric property of the FPIs was mainly attributed to the introduction of bulky pendant groups (isopropyl, 4-trifluoromethylphenyl) and noncoplanar structure in the polymer chains, which loosen the packing density of polymer chains, and increased free volume of polymers, and then caused the decreased dielectric constants. Especially, the incorporation of the fluorine-containing groups into the polymer structure would lead to great benefits toward improving polymer dielectric performance. This resulted from the special characteristics of fluorine including low polarizability and a relatively larger free volume.

Hydrophobic properties

As shown in Figure 10, the obtained contact angles were used to evaluate the hydrophobic properties of the FPIs, and the results were listed in Table 4. Obviously, compared with commercial Kapton film (Kapton, $\theta_w = 81.6°$), the FPI films presented remarkable hydrophobic properties with the contact angles in range of 87.3–93.9° due to the introduction of hydrophobic alkyl moieties (isopropyl) and fluorinated groups (trifluoromethyl). In particular, the high electronegativity characteristics of fluorine atom could reduce the surface energy of polymer, and then improved the hydrophobicity of polymers greatly. Obviously, PI-6FDA exhibited the best hydrophobicity among the polymers ($\theta_w = 93.9°$), and it may be due to the incorporation

of fluorine-containing groups from dianhydride moieties (6FDA).

Conclusions

Firstly, a novel aromatic fluorinated diamine PAPFT was synthesized, and then used to prepare a series of FPIs with various commercial dianhydrides by conventional one-step method. All of the FPIs presented excellent solubility in most organic solvents, good optical transparency, high thermal stability, outstanding mechanical properties, low dielectric constants and prominent hydrophobicity. The excellent comprehensive performance of FPIs might have the potential application for gas separation, polymeric waveguides, photoelectric and microelectronic materials.

Declaration of conflicting interests

The author(s) declared no potential conflicts of interest with respect to the research, authorship, and/or publication of this article.

Funding

The author(s) disclosed receipt of the following financial support for the research, authorship, and/or publication of this article: This work was financially supported by the National Natural Science Foundation of China (nos. 51563005, 51163003 and 21264005), the fund of Guangxi Natural Science Foundation (nos. 2014GXNSFAA118040 and 2013GXNSFDA019008), Guangxi Ministry-Province Jointly-Constructed Cultivation Base for State Key Laboratory of Processing for Non-ferrous Metal and Featured Materials (13KF-3), and Guangxi Funds for Specially-appointed Expert.

References

1. Ohya H, Kudryavtsev VV and Semenova SI. *Polyimide membranes: applications, fabrications, and properties*. Tokyo: Kodansha, 1996.
2. Ding MX. Isomeric polyimide. *Prog Polym Sci* 2007; **32**: 623–668.
3. Liaw DJ, Wang KL, Huang YC, et al. Advanced polyimide materials: syntheses, physical properties and applications. *Prog Polym Sci* 2012; **37**: 907–974.
4. Li XB, Song Y, Liu Z, et al. Triple-layer sulfonated poly(ether ether ketone)/sulfonated polyimide membranes for fuel cell applications. *High Perform Polym* 2014; **26**: 106–113.
5. Ghosh A, Sen SK, Banerjee S, et al. Solubility improvements in aromatic polyimides by macromolecular engineering. *RSC Adv* 2012; **2**: 5900–5926.
6. Xu HY, Yang HX, Tao LM, et al. Preparation and properties of glass cloth-reinforced meltable thermoplastic polyimide composites for microelectronic packaging substrates. *High Perform Polym* 2010; **22**: 581–597.
7. Liu CJ, Mei M, Pei XL, et al. Aromatic polyimides with tertbutyl-substituted and pendent naphthalene units: synthesis and soluble, transparent properties. *Chin J Polym Sci* 2015; **33**: 1074–1085.
8. Liu CJ, Pei XL, Huang XH, et al. Novel non-coplanar and tertbutyl-substituted polyimides: solubility, optical, thermal and dielectric properties. *Chin J Chem* 2015; **33**: 277–284.
9. Huang XH, Mei M, Liu CJ, et al. Synthesis and characterization of novel highly soluble and optical transparent polyimides containing tert-butyl and morpholinyl moieties. *J Polym Res* 2015; **22**: 169–177.
10. Yan SY, Chen WQ, Yan W, et al. Optical transparency and light colour of highly soluble fluorinated polyimides derived from a novel pyridine-containing diamine m, p-3FPAPP and various aromatic dianhydrides. *Des Monomers Polym* 2011; **14**: 579–592.
11. Sen SK and Banerjee S. Spiro-biindane containing fluorinated poly(ether imide)s: synthesis, characterization and gas separation properties. *J Membr Sci* 2010; **365**: 329–340.
12. Calle M, Lozano AE, de La Campa JG, et al. Novel aromatic polyimides derived from 5'-t-Butyl-2'-pivaloylimino-3,4,3'',4''-m-terphenyltetracarboxylic dianhydride with potential application on gas separation processes. *Macromolecules* 2010; **43**: 2268–2275.
13. Yi L, Li CY, Huang W, et al. Soluble aromatic polyimides with high glass transition temperature from benzidine containing tert-butyl groups. *J Polym Res* 2014; **21**: 572–581.
14. Gong SM, Liu M, Xia SL, et al. Synthesis of novel soluble polyimides containing triphenylamine groups for liquid crystal vertical alignment layers. *J Polym Res* 2014; **21**: 542–552.
15. Lin CH, Wong TI, Wang MW, et al. Synthesis of diallyl-containing polyimide and the effect of allyl groups on properties. *J Polym Sci A Polym Chem* 2015; **53**: 513–520.
16. Huang XH, Huang W, Liu JY, et al. Synthesis of highly soluble and transparent polyimides. *Polym Int* 2012; **61**: 1503–1509.
17. Zhang SJ, Li YF, Ma T, et al. Organosolubility and optical transparency of novel polyimides derived from 2',7'-bis(4-aminophenoxy)-spiro(fluorene-9,9'-xanthene). *Polym Chem* 2010; **1**: 485–493.
18. Thiruvasagam P. Synthesis of new unsymmetrical diamine and polyimides: structure-property relationship and applications of polyimides. *J Polym Res* 2012; **19**: 9965–9974.
19. Jiang GM, Jiang X, Zhu YF, et al. Synthesis and characterization of organo-soluble polyimides derived from a new spirobifluorene diamine. *Polym Int* 2010; **59**: 896–900.
20. Huang YC, Wang KL, Lee WY, et al. Novel heterocyclic poly(pyridine-imide)s with unsymmetric carbazole substituent and noncoplanar structure: high thermal, mechanical and optical transparency, electrochemical, and electrochromic properties. *J Polym Sci A Polym Chem* 2015; **53**: 405–412.
21. Barzic AI, Stoica I, Fifere N, et al. Morphological effects on transparency and absorption edges of some semi-alicyclic polyimide. *J Polym Res* 2013; **20**: 130–137.
22. Chang CW, Yen HJ, Huang KY, et al. Novel Organosoluble aromatic polyimides bearing pendant methoxy-substituted triphenylamine moieties: synthesis, electrochromic, and gas separation properties. *J Polym Sci A Polym Chem* 2008; **46**: 7937–7949.

23. Gao YF, Zhou YM, He M, et al. Synthesis and characterization of fluorinated polyimides derived from 1,4-bis-[4-amino-2-(trifluoromethyl)-phenoxy] benzene/tetrafluoride benzene. *Des Monomers Polym* 2014; **17**: 590–600.
24. Gao H, Yorifuji D, Jiang ZH, et al. Thermal and optical properties of hyperbranched fluorinated polyimide/mesoporous SiO_2 nanocomposites exhibiting high transparency and reduced thermo-optical coefficients. *Polymer* 2014; **55**: 2848–2855.
25. Chung CL, Lee WF, Lin CH, et al. Highly soluble fluorinated polyimides based on an asymmetric bis(ether amine): 1,7-bis(4-amino-2-trifluoromethylphenoxy)naphthalene. *J Polym Sci A Polym Chem* 2009; **47**: 1756–1770.
26. Ghosh A, Banerjee S and Voit B. Synthesis and characterization of new fluorinated polyimides derived from 9,10-bis[3'-trifluoromethyl-4'(4''-aminobenzoxy) benzyl] anthracene. *High Perform Polym* 2009; **21**: 173–186.
27. Cao XY, Jing LW, Liu YY, et al. Immiscible blends of sulfonated polyetheretherketone and fluorinated polyimide for proton exchange membranes. *High Perform Polym* 2014; **26**: 532–539.
28. Tapaswi PK, Choi MC, Nagappan S, et al. Synthesis and characterization of highly transparent and hydrophobic fluorinated polyimides derived from perfluorodecylthio substituted diamine monomers. *J Polym Sci A Polym Chem* 2015; **53**: 479–488.
29. Yang CP, Su YY and Chiang HC. Organosoluble and light-colored fluorinated polyimides from 4-tert-butyl-[1,2-bis(4-amino-2-trifluoromethylphenoxy)phenyl] benzene and aromatic dianhydrides. *React Funct Polym* 2006; **66**: 689–701.
30. Matsumoto T and Kurosaki T. Soluble and colorless polyimides from bicyclo[2.2.2]octane-2,3,5,6-tetracarboxylic 2,3:5,6-dianhydrides. *Macromolecules* 1997; **30**: 993–1000.
31. Wang LD, Zhang T, Li RZ, et al. Synthesis and characterization of cross-linkable fluorinated polyimide for optical waveguide. *Appl Phys A Mater* 2015; **118**: 655–664.
32. Shundrina IK, Vaganova TA, Kusov SZ, et al. Synthesis and properties of organosoluble polyimides based on novel perfluorinated monomer hexafluoro-2,4-toluenediamine. *J Fluorine Chem* 2011; **132**: 207–215.